

Revealing multiple density wave orders in nonsuperconducting titanium oxypnictide $\text{Na}_2\text{Ti}_2\text{As}_2\text{O}$

Y. Huang, H. P. Wang, R. Y. Chen, X. Zhang, P. Zheng, Y. G. Shi, and N. L. Wang*

Beijing National Laboratory for Condensed Matter Physics, Institute of Physics, Chinese Academy of Sciences, Beijing 100190, China

(Received 19 January 2014; revised manuscript received 4 April 2014; published 14 April 2014)

We report an optical spectroscopy study on single crystals of $\text{Na}_2\text{Ti}_2\text{As}_2\text{O}$, a sister compound of the superconductor $\text{BaTi}_2\text{Sb}_2\text{O}$. The study unexpectedly reveals two density wave phase transitions. The first transition, at 320 K, results in the formation of a large energy gap and removes the majority of the Fermi surfaces. But the compound remains metallic with residual itinerant carriers. Below 42 K, another density wave phase transition with a smaller energy gap scale occurs and drives the compound into the semiconducting ground state. These experiments thus enable us to shed light on the complex electronic structure in titanium oxypnictides.

DOI: [10.1103/PhysRevB.89.155120](https://doi.org/10.1103/PhysRevB.89.155120)

PACS number(s): 71.45.Lr, 74.25.Gz, 74.70.-b, 75.30.Fv

The low-temperature broken-symmetry states in low-dimensional materials, such as superconductivity, charge density waves (CDWs), and spin density waves (SDWs), are among the most fascinating collective phenomena in solids and the interplay between them has been a subject of considerable interest in condensed matter physics [1–6]. Most density-wave (DW) instabilities (either CDWs or SDWs) are driven by the nesting topology of Fermi surfaces (FSs) where the electronic susceptibility has a divergence at the nesting wave vector. Brought about by electron-phonon or electron-electron interactions, a single particle energy gap opens in the nested regions of FSs, resulting in the lowering of the electronic energy of the system. In one-dimensional (1D) system the DW phase transition usually causes an semiconducting ground state due to the opening of a full energy gap arising from the perfect nesting of FSs. However, for two-dimensional (2D) or three-dimensional (3D) materials, the CDW or SDW ground states mostly remain metallic due to the formation of partial energy gap induced by the imperfect nesting of FSs. To date, there seems no reported example of a truly semiconducting ground state caused by the DW phase transition in a 2D or 3D system.

Recently, a new superconducting system $\text{Ba}_{1-x}\text{Na}_x\text{Ti}_2\text{Sb}_2\text{O}$ ($T_c \sim 2\text{--}5$ K) has attracted much attention [7–9]. The system belongs to a two-dimensional (2D) titanium oxypnictide family, consisting of alternate stacking of conducting octahedral layers $\text{Ti}_2\text{Pn}_2\text{O}$ (Pn = As, Sb) and other insulating layers [e.g., Na_2 , Ba, $(\text{SrF})_2$, $(\text{SmO})_2$] [9–18]. The undoped compounds in this family commonly exhibit phase transitions below certain temperatures (e.g., 114 K for $\text{Na}_2\text{Ti}_2\text{Sb}_2\text{O}$ [12], 320 K for $\text{Na}_2\text{Ti}_2\text{As}_2\text{O}$ [11–14, 16], 45 K for $\text{BaTi}_2\text{Sb}_2\text{O}$ [7], 200 K for $\text{BaTi}_2\text{As}_2\text{O}$ [17]), as characterized by the sharp jumps in resistivity and drops in magnetic susceptibility. First-principle band structure calculations indicate that the phase transitions are driven by the DW instabilities arising from the nested electron and hole FSs [19–23]. As superconductivity emerges only in compounds with a low phase transition temperature and T_c is further enhanced when the phase transition temperature is suppressed by doping, the family offers a new playground to study the interplay between superconductivity and DW instabilities. Understanding the electronic properties in the undoped compounds is an essential step towards

understanding the superconductivity in this family. Among the different members in the family, $\text{Na}_2\text{Ti}_2\text{As}_2\text{O}$ appears to be particularly interesting. First-principle calculations indicate that the compound has an SDW ground state with a blocked checkerboard antiferromagnetic order, and the ordered state is not metallic but semiconducting, with an energy gap of 0.15 eV [22]. Up to the present, there have been few experimental studies on this material. It is highly desirable to probe its electronic properties and, in particular, to examine whether such an semiconducting ground state is really realized in the $\text{Na}_2\text{Ti}_2\text{As}_2\text{O}$ system.

In this work we present an optical spectroscopic study on $\text{Na}_2\text{Ti}_2\text{As}_2\text{O}$ single crystals. Unexpectedly, the study reveals two DW phase transitions for the compound. The first one, at high temperatures (~ 320 K), results in the formation of a large DW energy gap with $2\Delta = 2600$ cm and removes most of the FSs. But the compound retains a metallic nature after this phase transition. Below 42 K, another DW gap forms and removes the rest of the FSs completely. Such two-step phase transitions, which eventually lead to a semiconducting ground state, were not anticipated from the first-principle calculation. $\text{Na}_2\text{Ti}_2\text{As}_2\text{O}$ manifests much more complexly than one would expect. It is likely to be a rare example of a quasi-2D material undergoing the metal-insulator (M-I) transition driven by DW instability.

Single-crystal samples of $\text{Na}_2\text{Ti}_2\text{As}_2\text{O}$ used in this study were grown by the NaAs flux method [24]. Figure 1 shows the in-plane temperature-dependent resistivity and magnetic susceptibility measured in a Quantum Design physical property measurement system and a superconducting quantum interference device vibrating sample magnetometer, respectively. Clear anomalies are observed near 320 K, where the resistivity displays a rapid increase and the magnetic susceptibility a sharp drop. Below the phase transition, the resistivity keeps increasing with decreasing temperature, reaches a maximum near 150 K, then decreases slightly. But below roughly 50 K, the resistivity goes up sharply and the compound becomes semiconducting like at the lowest temperature. Such a behavior has not been observed in any other member of the titanium oxypnictide family. In the magnetic susceptibility curve, a weak kink is seen near 42 K, suggesting the emergence of another phase transition. Those anomalies were repeatedly observed in different samples. As will be seen below, optical spectroscopy measurement revealed clearly two distinct DW phase transitions.

*nlwang@aphy.iphy.ac.cn

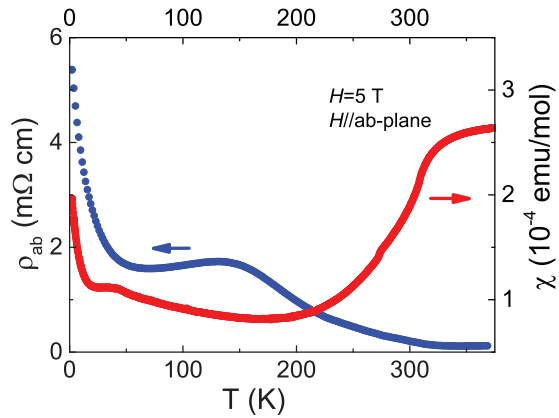


FIG. 1. (Color online) Temperature-dependent in-plane resistivity and magnetic susceptibility of $\text{Na}_2\text{Ti}_2\text{As}_2\text{O}$.

Figure 2 and 3 show the reflectance $R(\omega)$ and real part of conductivity $\sigma_1(\omega)$ spectra at different temperatures. The insets show $R(\omega)$ and $\sigma_1(\omega)$ spectra on a linear frequency scale. The measurement technique is the same as we presented before [25]. At 330 K, a temperature higher than the phase transition, $R(\omega)$ shows a typical metallic response. $R(\omega)$ approaches unity at zero frequency and drops almost linearly with increasing frequency. This well-known overdamped behavior indicates rather strong carrier scattering. A striking feature is that $R(\omega)$ is strongly suppressed below 2600 cm^{-1} below the phase transition temperature at $T_1 = 320\text{ K}$. Accordingly, a remarkable peak structure emerges in $\sigma_1(\omega)$ and becomes more pronounced upon cooling (left inset in Fig. 3). It is a typical DW energy gap character in the optical conductivity spectrum, which is determined by the “type I coherent factor” for DW order [26,27]. The spectral change across the phase transition is rather similar to that seen for its sister compound $\text{Na}_2\text{Ti}_2\text{Sb}_2\text{O}$, where the phase transition occurs at 114 K [25]. The peak position in $\sigma_1(\omega)$ roughly gives the gap value of

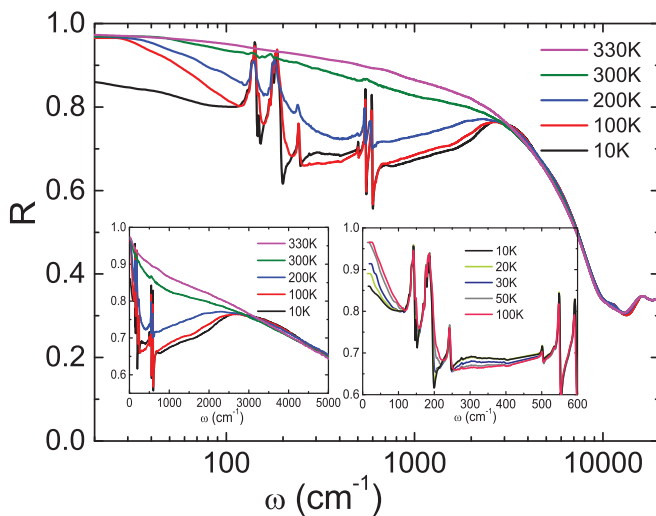


FIG. 2. (Color online) $R(\omega)$ spectra for $\text{Na}_2\text{Ti}_2\text{As}_2\text{O}$ at several representative temperatures. Left inset: $R(\omega)$ spectra up to 5000 cm^{-1} on a linear frequency scale. Right inset: $R(\omega)$ spectra up to 600 cm^{-1} at low temperatures.

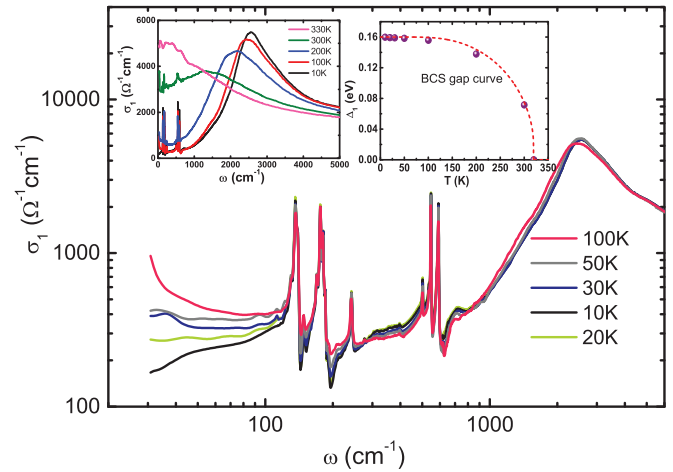


FIG. 3. (Color online) $\sigma_1(\omega)$ spectra for $\text{Na}_2\text{Ti}_2\text{As}_2\text{O}$ at low temperatures over a broad range of frequencies. Left inset: Conductivity spectra up to 5000 cm^{-1} on a linear frequency scale. Right inset: Plot of energy gap Δ_1 , extracted from the optical measurement, as a function of temperature. Data points follow the curve of BCS theory for a density-wave phase transition (dashed curve).

$2\Delta_1 = 2600\text{ cm}^{-1}$ ($\sim 0.32\text{ eV}$). This leads to the ratio of the energy gap relative to the transition temperature $2\Delta_1/k_B T_1 \approx 11.5$ at 10 K . The value is also close to that obtained for the $\text{Na}_2\text{Ti}_2\text{Sb}_2\text{O}$ compound [25]. Notably, this value is much larger than the BCS (Bardeen-Cooper-Schrieffer) mean-field value of 3.52 for a DW phase transition [1]. This means that the transition temperature is significantly lower than the mean-field transition temperature. It might be due to the highly 2D electronic structure, which leads to a strong fluctuation effect and suppresses the actual ordering temperature. The 2D nature of the compound is well supported by the large value of the anisotropic ratio of the resistivities, $\rho_c(T)/\rho_{ab}(T) \sim 400$ [24]. Similar gap ratios were also observed in other low-dimensional DW materials, e.g., $(\text{TaSe}_4)_2\text{I}$ [1]. The right inset in Fig. 3 shows the plot of the energy gap Δ_1 , extracted from the optical measurement, as a function of the temperature. The data points follow the curve of BCS theory for a DW phase transition, implying that the transition is a second-order phase transition. It should be emphasized that the low- ω $R(\omega)$ in the DW ordered state increases more rapidly towards unity at zero frequency than that at 330 K . As a consequence, one can see a rather sharp low- ω reflectance edge. This indicates clearly that the FSs are only partially gapped and the compounds are still metallic below T_s .

Surprising results were observed at low temperatures. As shown in the right inset in Fig. 2, below 50 K , a new suppression feature appears in $R(\omega)$ at a much lower energy scale, roughly below 300 cm^{-1} . Above this energy level, there is a slight enhancement of reflectance. This character becomes more pronounced as the temperature decreases. It is very similar to the spectral change arising from the opening of the DW energy gap as we have explained for the phase transition at 320 K . In the $\sigma_1(\omega)$ spectra, the suppression of conductivity at low frequency could be clearly seen below 50 K . Nevertheless, due to the emergence of strong phonon modes, the peak position could not be unambiguously resolved. Overall, this

second gap feature is much weaker than the first one at 320 K. This could be attributed to the small residual carrier density being left after the first DW phase transition. Judging from the suppression frequency in $R(\omega)$ and the spectral weight (SW) analysis as presented below, the gap value is estimated to be about $2\Delta_2 = 300 \text{ cm}^{-1}$. Combined with the anomalies in resistivity and magnetic susceptibility at $T_2 = 42 \text{ K}$, the observation yields compelling evidence for the development of a new DW order. From the gap value, we obtained the ratio of the energy gap relative to the transition temperature $2\Delta_2/k_B T_2 \sim 10$ for the second transition, which is similar to the value for the first DW phase transition. It is noteworthy that the earlier measurement of the anisotropic ratio of resistivities by the Montgomery technique on $\text{Na}_2\text{Ti}_2\text{As}_2\text{O}$ showed a very sharp drop below 50 K [24], implying the reconstruction of band structure at low temperature, while no such abrupt change in anisotropic resistivities was seen in $\text{Na}_2\text{Ti}_2\text{Sb}_2\text{O}$ crystals. These anisotropic resistivity data also support the presence of the second phase transition below 50 K.

At 10 K, the lowest measurement temperature, the reflectance value is finite and smaller than unity at the zero-frequency limit. In $\sigma_1(\omega)$, the Drude component is absent and phonon structures become dominant. The very small low-frequency SW is likely due to the effect of the finite measurement temperature (10 K). The results indicate that, in the ground state, the FSs are fully gapped and the compound becomes a semiconductor. In 2D DW materials, one usually observes enhanced metallic behavior below the transition because the partial DW energy gap tends to remove the electrons that experience stronger scattering [28]. Although there are a few examples of nonmetallic 2D CDW systems, the origin of the semiconducting behavior is actually due not to true FS nesting but to Mott physics [29–31]. LaTe_2 was suggested to be a 2D FS-nesting-driven semiconducting CDW system [32], however, a more recent study indicated that the nonmetallic behavior is in fact caused by the localization effect due to the presence of defects in conducting Te layers [33]. In this regard, $\text{Na}_2\text{Ti}_2\text{As}_2\text{O}$ may be a good candidate of FS-nesting-driven semiconducting material.

To analyze the evolution of both the itinerant carriers and the DW gap excitations in a quantitative way, we use a Drude-Lorentz mode to fit the optical spectra in a broad frequency range [26]:

$$\epsilon(\omega) = \epsilon_\infty - \frac{\omega_p^2}{\omega^2 + i\omega/\tau_D} + \sum_{i=1}^N \frac{S_i^2}{\omega_i^2 - \omega^2 - i\omega/\tau_i}. \quad (1)$$

Here, the ϵ_∞ is the dielectric constant at high energy, and the middle and last terms are the Drude and Lorentz components, respectively. From the relationship between the conductivity and the dielectric function $\epsilon(\omega) = \epsilon_\infty + \frac{4\pi i}{\omega} \sigma(\omega)$, the real part of the conductivity has the form

$$\sigma_1(\omega) = \frac{\omega_p^2}{4\pi} \frac{1/\tau_D}{\omega^2 + 1/\tau_D^2} + \sum_{i=1}^N \frac{S_i^2}{4\pi} \frac{\omega^2/\tau_i}{(\omega_i^2 - \omega^2)^2 + \omega^2/\tau_i^2}. \quad (2)$$

The Drude term captures the contribution from free carriers and the Lorentz components describe the excitations across the gap and interband transitions. It is found that the experimental data below 5000 cm^{-1} at 330 K could be reproduced

TABLE I. Temperature dependence of the plasma frequency ω_p and scattering rate $\gamma_D = 1/\tau_D$ of the Drude term, the resonance frequency ω_i , the width $\gamma_i = 1/\tau_i$, and the square root of the oscillator strength S_i of the Lorentz component (all entries in 10^3 cm^{-1}). One Drude mode is employed at high temperatures. Lorentz terms responsible for the DW orders are added at low temperatures. The lowest energy interband transition is also displayed.

	ω_p	γ_D	ω_1	γ_1	S_1	ω_2	γ_2	S_2	ω_3	γ_3	S_3
330 K	23	2	5	8	23	—	—	—	—	—	—
300 K	13	1	5.4	8	23	1.2	2.5	20	—	—	—
200 K	4.1	0.3	5.4	7.5	23	2.2	1.9	22	—	—	—
100 K	2.4	0.1	5.4	7.5	23	2.5	1.8	22.7	—	—	—
50 K	2.3	0.09	5.4	7.5	23	2.6	1.6	22.5	—	—	—
10 K	—	—	5.4	7.5	23	2.6	1.5	21.5	0.3	0.44	2.6

approximately by one Drude term and one Lorentz component (Lorentz S_1 term). After the first phase transition, another Lorentz peak, S_2 (DW gap 1), is added. As the temperature is lowered below 42 K, a third Lorentz term, S_3 (DW gap 2), develops and takes the place of the Drude component completely. A list of fitting parameters is reported in Table I. The fitting results for three representative temperatures are shown in Fig. 4. It illustrates clearly that the compound undergoes two phase transitions with different energy gap scales.

It is noteworthy that the plasma frequency at 330 K (above the first phase transition) is about $23\,000 \text{ cm}^{-1}$, which is almost equal to that of $\text{Na}_2\text{Ti}_2\text{Sb}_2\text{O}$, while $1/\tau \approx 2000 \text{ cm}^{-1}$ is much larger than that of $\text{Na}_2\text{Ti}_2\text{Sb}_2\text{O}$ [25]. This explains the higher resistivity values of the $\text{Na}_2\text{Ti}_2\text{As}_2\text{O}$ compound. The variations in plasma frequency and scattering rate $1/\tau$ normalized to the values at 330 K as a function of the temperature are displayed in the lower-right panel in Fig. 4. Provided that the effective mass of itinerant carriers does not change with temperature, the residual carrier density at 100 K is only 10% of that at high temperature. Meanwhile, the scattering rate also decreases by 90%. This indicates that the opening of the partial DW gap removes the electrons near the Fermi level which bear stronger scattering. This character is similar to $\text{Na}_2\text{Ti}_2\text{Sb}_2\text{O}$, but the scattering rate of $\text{Na}_2\text{Ti}_2\text{As}_2\text{O}$ is less reduced. These evolutions agree well with the temperature dependence of resistivity. The itinerant carrier density becomes 0 at the lowest temperature, suggesting that the residual FS has been fully gapped by the second DW order.

A SW analysis gives more insight into the development of the two orders. The SW shown in Fig. 5 is defined as $W_s = \int_0^{\omega_c} \sigma_1(\omega) d\omega$, where ω_c is the cutoff frequency. The small step structures below 200 K in the low-frequency region, between 100 and 600 cm^{-1} , are ascribed to the phonons. At very low energy, the W_s at 330 K has the highest value due to the large Drude component. Below 300 K, the SW is severely suppressed at about 2000 cm^{-1} and recovered at a higher energy. This indicates the formation of an energy gap. Moreover, another suppression in the low- ω region becomes eminent at 20 and 10 K. The SW approaches approximately 0 at finite frequency at 10 K, indicating its insulator character. The suppression is an indication of the second energy gap opening, which leads to the M-I transition. We note that the spectral curvatures of W_s near $200\text{--}300 \text{ cm}^{-1}$ at 10 and 20 K

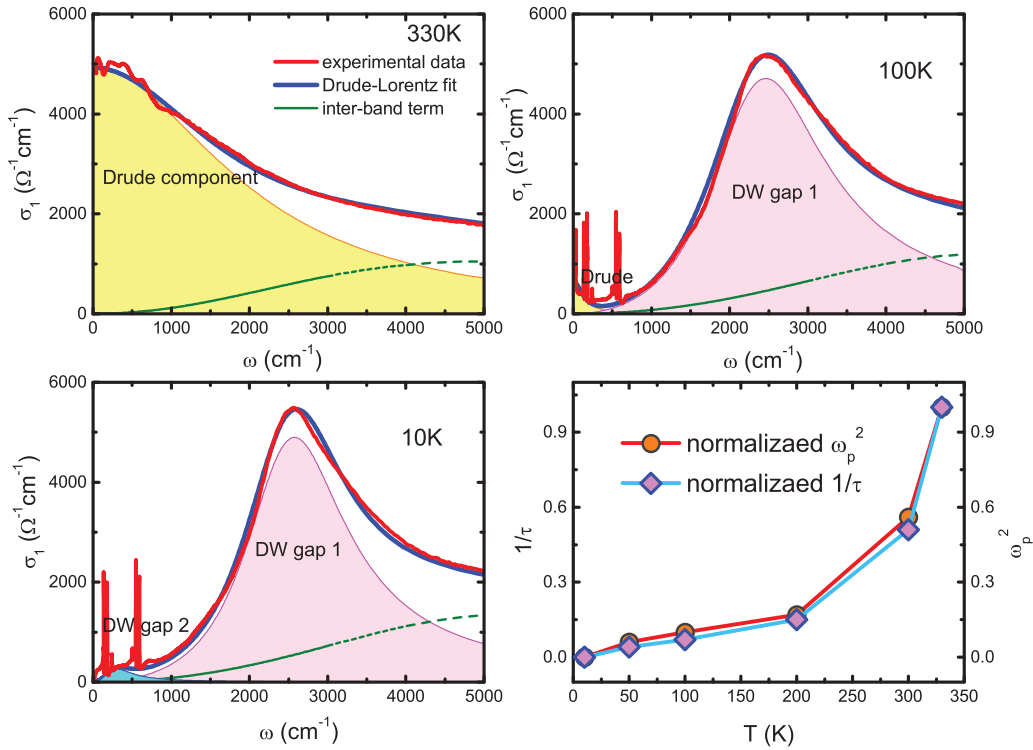


FIG. 4. (Color online) Experimental data on $\sigma_1(\omega)$ at 330, 100, and 10 K together with Drude-Lorentz fits. Lower right panel: Variations of $1/\tau$ and ω_p^2 normalized to the values at 330 K as a function of temperature.

are rather similar to the those near 2000–3000 cm^{-1} at 100 and 200 K, as indicated by the two arrows in Fig. 5. Therefore, the temperature dependence of the SW suppression reflects two different DW energy gap openings below 320 and 42 K, respectively.

The observation of two DW phase transitions is totally unexpected. Although an FS-nesting-driven SDW semiconducting ground state is obtained from the first-principle calculations [22], the experimental observations differ in two aspects. First, the two-step phase transitions were not

anticipated from the calculations. Second, the value of the energy gap in the ordered state from first-principle calculations (0.15 eV) is only half of the gap value observed for the first DW phase transition, but four times larger than that for the second DW phase transition. Apparently, further theoretical work is needed to resolve this discrepancy. A more realistic approach to the ground state is first to consider a metastable intermediate DW state driven probably by the strongest nesting instability of FSs and then to examine further possible instability on the basis of the intermediate DW state.

It also deserves remark that, although the optical measurement revealed the formation of two energy gaps at different temperatures, the measurement could not determine where the FSs are gapped. A momentum-resolved experimental probe, such as angle-resolved photoemission, should be used to determine the gapped regions and corresponding wave vectors. Another important issue is that, although the optical experiment indicated typical DW phase transitions, the measurement could not determine whether the phase transitions were CDWs or SDWs since both orders have the same coherent factor and, therefore, the same energy gap character. Other techniques that are capable of probing magnetism should be used to resolve the issue. A recent NMR measurement on a $\text{BaTi}_2\text{Sb}_2\text{O}$ polycrystalline sample revealed the absence of an internal field at the Sb site, which therefore favored an CDW origin [34]. Nevertheless, this result is actually in agreement with the first-principle calculations, which indeed predicted a CDW ground state for $\text{BaTi}_2\text{Sb}_2\text{O}$ [23]. On the contrary, the first-principle calculations on $\text{Na}_2\text{Ti}_2\text{As}_2\text{O}$ indicated a semiconducting SDW ground state with a blocked antiferromagnetic order [22]. Therefore, sensitive magnetic

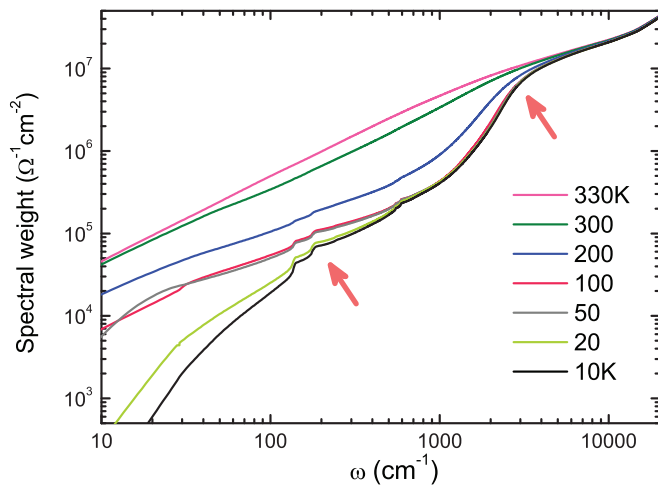


FIG. 5. (Color online) Frequency-dependent spectral weight at different temperatures. Curvatures indicated by arrows reflect the effect of spectral weight redistributions caused by DW gap openings.

probes should be applied particularly to the $\text{Na}_2\text{Ti}_2\text{As}_2\text{O}$ compound. Resolving those issues is of great significance in view of the profound relationship between the DW (SDW or CDW) and superconductivity in this family. The present study is expected to motivate more experimental and theoretical studies on these materials.

To conclude, we have studied the in-plane optical properties of $\text{Na}_2\text{Ti}_2\text{As}_2\text{O}$ single crystals, a sister compound of the superconductor $\text{BaTi}_2\text{Sb}_2\text{O}$. Unexpectedly, the study revealed two DW phase transitions. The first transition, at 320 K, results in the formation of a large energy gap and removal of most of the FSs. The second phase transition, with a smaller energy

gap scale, occurs below 42 K and drives the compound into the semiconducting ground state. This makes $\text{Na}_2\text{Ti}_2\text{As}_2\text{O}$ a quasi-2D DW semiconductor driven by FS nesting as in 1D materials. The study sheds light on the complex electronic structures of titanium oxypnictides.

The authors acknowledge useful discussions with Z. Y. Lu and J. L. Luo. This work was supported by the National Science Foundation of China (Grants No. 11120101003 and No. 11327806) and the 973 project of the Ministry of Science and Technology of China (Grants No. 2011CB921701 and No. 2012CB821403).

-
- [1] G. Grüner, *Density Waves in Solids* (Addison-Wesley, Reading, MA, 1994).
- [2] J. A. Wilson and A. D. Yoffe, *Adv. Phys.* **18**, 193 (1969).
- [3] J. A. Wilson, *Phys. Rev. B* **15**, 5748 (1977).
- [4] P. Mongeau, N. P. Ong, A. M. Portis, A. Meerschaut, and J. Rouxel, *Phys. Rev. Lett.* **37**, 602 (1976).
- [5] B. Becker, N. G. Patil, S. Ramakrishnan, A. A. Menovsky, G. J. Nieuwenhuys, J. A. Mydosh, M. Kohgi, and K. Iwasa, *Phys. Rev. B* **59**, 7266 (1999).
- [6] L. Degiorgi, M. Dressel, A. Schwartz, B. Alavi, and G. Grüner, *Phys. Rev. Lett.* **76**, 3838 (1996).
- [7] T. Yajima, K. Nakano, F. Takeiri, T. Ono, Y. Hosokoshi, Y. Matsushita, J. Hester, Y. Kobayashi, and H. Kageyama, *J. Phys. Soc. Jpn.* **81**, 103706 (2012).
- [8] P. Doan, M. Gooch, Z. Tang, B. Lorenz, A. Möller, J. Tapp, P. C. W. Chu, and A. M. Guloy, *J. Am. Chem. Soc.* **134**, 16520 (2012).
- [9] H. F. Zhai, W.-H. Jiao, Y.-L. Sun, J.-K. Bao, H. Jiang, X.-J. Yang, Z.-T. Tang, Q. Tao, X.-F. Xu, Y.-K. Li, C. Cao, J.-H. Dai, Z.-A. Xu, and G.-H. Cao, *Phys. Rev. B* **87**, 100502(R) (2013).
- [10] A. Adam and H.-U. Schuster, *Z. Anorg. Allg. Chem.* **584**, 150 (1990).
- [11] E. A. Axtell, III, T. Ozawa, S. M. Kauzlarich, and R. R. P. Singh, *J. Solid State Chem.* **134**, 423 (1997).
- [12] T. C. Ozawa, R. Pantoja, E. A. Axtell, S. M. Kauzlarich, J. E. Greedan, M. Bieringer, and J. W. Richardson, *J. Solid State Chem.* **153**, 275 (2000).
- [13] T. C. Ozawa, S. M. Kauzlarich, M. Bieringer, and J. E. Greedan, *J. E. Chem. Mater.* **13**, 1804 (2001).
- [14] T. C. Ozawa and S. M. Kauzlarich, *J. Cryst. Growth* **265**, 571 (2004).
- [15] T. C. Ozawa and S. M. Kauzlarich, *Sci. Technol. Adv. Mater.* **9**, 033003 (2008).
- [16] R. H. Liu, D. Tan, Y. A. Song, Q. J. Li, Y. J. Yan, J. J. Ying, Y. L. Xie, X. F. Wang, and X. H. Chen, *Phys. Rev. B* **80**, 144516 (2009).
- [17] X. F. Wang, Y. J. Yan, J. J. Ying, Q. J. Li, M. Zhang, N. Xu, and X. H. Chen, *J. Phys.: Condens. Matter* **22**, 075702 (2010).
- [18] R. H. Liu, Y. A. Song, Q. J. Li, J. J. Ying, Y. J. Yan, Y. He, and X. H. Chen, *Chem. Mater.* **22**, 1503 (2010).
- [19] W. E. Pickett, *Phys. Rev. B* **58**, 4335 (1998).
- [20] F. F. de Biani, P. Alemany, and E. Canadell, *Inorg. Chem.* **37**, 5807 (1998).
- [21] D. J. Singh, *New J. Phys.* **14**, 123003 (2012).
- [22] X. W. Yan and Z. Y. Lu, *J. Phys.: Condens. Matter* **25**, 365501 (2013).
- [23] A. Subedi, *Phys. Rev. B* **87**, 054506 (2013).
- [24] Y. G. Shi, H. P. Wang, X. Zhang, W. D. Wang, Y. Huang, and N. L. Wang, *Phys. Rev. B* **88**, 144513 (2013).
- [25] Y. Huang, H. P. Wang, W. D. Wang, Y. G. Shi, and N. L. Wang, *Phys. Rev. B* **87**, 100507(R) (2013).
- [26] W. Z. Hu, J. Dong, G. Li, Z. Li, P. Zheng, G. F. Chen, J. L. Luo, and N. L. Wang, *Phys. Rev. Lett.* **101**, 257005 (2008).
- [27] M. Dressel and G. Grüner, *Electrodynamics of Solids: Optical Properties of Electrons in Matter* (Cambridge University Press, Cambridge, UK, 2002).
- [28] W. Z. Hu, G. Li, J. Yan, H. H. Wen, G. Wu, X. H. Chen, and N. L. Wang, *Phys. Rev. B* **76**, 045103 (2007).
- [29] S. Colonna, F. Ronci, A. Cricenti, L. Perfetti, H. Berger, and M. Grioni, *Phys. Rev. Lett.* **94**, 036405 (2005).
- [30] J. J. Kim, W. Yamaguchi, T. Hasegawa, and K. Kitazawa, *Phys. Rev. Lett.* **73**, 2103 (1994).
- [31] G. Cao, S. McCall, J. E. Crow, and R. P. Guertin, *Phys. Rev. Lett.* **78**, 1751 (1997).
- [32] D. R. Garcia, G.-H. Gweon, S. Y. Zhou, J. Graf, C. M. Jozwiak, M. H. Jung, Y. S. Kwon, and A. Lanzara, *Phys. Rev. Lett.* **98**, 166403 (2007).
- [33] Y. Huang, B. F. Hu, T. Dong, A. F. Fang, P. Zheng, and N. L. Wang, *Phys. Rev. B* **86**, 205123 (2012).
- [34] S. Kitagawa, K. Ishida, K. Nakano, T. Yajima, and H. Kageyama, *Phys. Rev. B* **87**, 060510(R) (2013).